NIH Public Access
Author Manuscript
Biochim Biophys Acta. Author manuscript; available in PMC 2009 June 29.

Published in final edited form as:
Biochim Biophys Acta. 2007 November ; 1768(11): 2690–2697. doi:10.1016/j.bbamem.2007.06.031.

Cloning and Functional Characterization of Human SMCT2 (SLC5A12) and Expression Pattern of the Transporter in Kidney

E. Gopal[a], **N. S. Umapathy**[a], **P. M. Martin**[a], **S. Ananth**[a], **J. P. Gnana-Prakasam**[a], **H. Becker**[b], **C. A. Wagner**[b], **V. Ganapathy**[a], and **P. D. Prasad**[a,*]

[a] *Department of Biochemistry and Molecular Biology, Medical College of Georgia, Augusta, Georgia, 30912, U.S.A* [b] *Institute of Physiology and Zurich Center for Integrative Human Physiology, University of Zurich, Zurich, Switzerland*

Abstract

Recently, we cloned two Na^+-coupled lactate transporters from mouse kidney, a high-affinity transporter (SMCT1 or slc5a8) and a low-affinity transporter (SMCT2 or slc5a12). Here we report on the cloning and functional characterization of human SMCT2 (SLC5A12) and compare the immunolocalization patterns of slc5a12 and slc5a8 in mouse kidney. The human SMCT2 cDNA codes for a protein consisting of 618 amino acids. When expressed in mammalian cells or *Xenopus* oocytes, human SMCT2 mediates Na^+-coupled transport of lactate, pyruvate and nicotinate. The affinities of the transporter for these substrates are lower than those reported for human SMCT1. Several non-steroidal anti-inflammatory drugs (NSAIDs) inhibit human SMCT2-mediated nicotinate transport, suggesting that NSAIDs interact with the transporter as they do with human SMCT1. Immunofluorescence microscopy of mouse kidney sections with an antibody specific for SMCT2 shows that the transporter is expressed predominantly in the cortex. Similar studies with an anti-SMCT1 antibody demonstrate that SMCT1 is also expressed mostly in the cortex. Dual-labeling of SMCT1 and SMCT2 with 4F2hc (CD98), a marker for basolateral membrane of proximal tubular cells in the S1 and S2 segments of the nephron, shows that both SMCT1 and SMCT2 are expressed in the apical membrane of the tubular cells. These studies also show that while SMCT2 is broadly expressed along the entire length of the proximal tubule (S1/S2/S3 segments), the expression of SMCT1 is mostly limited to the S3 segment. These studies suggest that the low-affinity transporter SMCT2 initiates lactate absorption in the early parts of the proximal tubule followed by the participation of the high-affinity transporter SMCT1 in the latter parts of the proximal tubule.

Keywords

kidney; proximal tubule; lactate reabsorption; nicotinate; immunolocalization

*Corresponding author: Dr. Puttur D. Prasad, Department of Biochemistry and Molecular Biology, Medical College of Georgia, Augusta, GA 30912-2100, U.S.A. Phone: 706-721-1761, Fax: 706-721-3891, E-mail: E-mail: pprasad@mail.mcg.edu.

Publisher's Disclaimer: This is a PDF file of an unedited manuscript that has been accepted for publication. As a service to our customers we are providing this early version of the manuscript. The manuscript will undergo copyediting, typesetting, and review of the resulting proof before it is published in its final citable form. Please note that during the production process errors may be discovered which could affect the content, and all legal disclaimers that apply to the journal pertain.

NIH-PA Author Manuscript
NIH-PA Author Manuscript
NIH-PA Author Manuscript

NIH-PA Author Manuscript

NIH-PA Author Manuscript

NIH-PA Author Manuscript

1. Introduction

Normal blood lactate levels are ~ 1.5 mM, but less than 5% of filtered lactate is excreted in the urine, suggesting the presence of efficient mechanisms for reabsorption of lactate in the kidney [1,2]. While Na^+-independent, H^+-coupled monocarboxylate transporters (MCTs) are known to play a major role in the transmembrane transfer of lactate in a variety of cells [3], lactate uptake in renal apical membrane vesicles occurs via Na^+-dependent processes [4,5]. Jorgensen and Sheikh, using apical membrane vesicles isolated from the outer and inner layers of rabbit kidney cortex, have provided evidence for the presence of two Na^+-dependent transport systems for monocarboxylates in the proximal tubule [6–9]. A low-affinity Na^+-coupled lactate transport system (Km ~40 mM) is expressed in the initial part (pars convoluta) of the proximal tubule and a high-affinity Na^+-coupled lactate transport system (Km ~0.25 mM) is expressed in the distal part (pars recta) of the proximal tubule [6].

The molecular identity of the high-affinity lactate transport system was recently revealed with the functional characterization of SLC5A8, also known as SMCT1 (Sodium-coupled MonoCarboxylate Transporter 1) [10–14]. SMCT1 transports lactate, pyruvate, butyrate, propionate, acetate and the B-complex vitamin nicotinate in a Na^+-coupled and electrogenic manner. The Km for SLC5A8-mediated lactate transport is ~0.25 mM, which agrees well with the values obtained for the high-affinity lactate transport system in apical membrane vesicles from pars recta. More recently, we cloned slc5a12 (SMCT2) from a mouse kidney cDNA library and characterized its transport function [15]. The mouse slc5a12 is structurally and functionally similar to mouse slc5a8. The two proteins share 59% identity and 75% similarity at the amino acid level. Functionally, slc5a12 mediates the transport of various monocarboxylates with low affinity (Km for lactate, ~35 mM), which agrees well with the values obtained for the low-affinity lactate transport system in apical membrane vesicles from pars convoluta. The mouse slc5a12-mediated transport process was Na^+-dependent and weakly electrogenic. Recently, we provided evidence for the obligatory nature of these two transporters in renal reabsorption of lactate in a mouse model (c/ebpδ null mice) which lack the expression of both transporters in kidney [16].

In this paper, we report on the cloning and functional characterization of human SMCT2. In addition, we have compared the expression patterns of SMCT1 and SMCT2 in mouse kidney. These studies show that human SMCT2 functions as a low-affinity Na^+-coupled transporter for monocarboxylates and that the transporter is indeed expressed in the apical membrane of the cells lining the initial segments of the proximal tubule. In contrast, the high-affinity Na^+-coupled lactate transporter SMCT1 is expressed in the apical membrane of the cells lining the late segments of the proximal tubule.

2. Materials and Methods

2.1. Cloning of the human SMCT2

Since there was no sequence information for human SMCT2 cDNA in GenBank, we first performed a Translated Blast (TBLASTN) search against the human genome database using the amino acid sequence of mouse SMCT2 as the query. The search identified a candidate gene for SMCT2 on human chromosome 11 (GenBank accession number NT_009237). Based on the predicted exons of the gene, sense and antisense primers were designed to clone the full-length human SMCT2 cDNA by RT-PCR using human kidney total RNA (Clontech). The sense primer, containing the initiation codon (shown in bold) and an artificial Kozak sequence (underlined), was 5′-GATATATAGCC**ATG**GAGGTGAAGAACTTTG-3′, and the antisense primer, located immediately downstream of the stop codon, was 5′-CGTCTAGATGTGCATTCATACAGGTATTG-3′. Engineered into the 5′-end of the antisense primer is an XbaI site (underlined), added to aid in the directional cloning of the

NIH-PA Author Manuscript

NIH-PA Author Manuscript

NIH-PA Author Manuscript

amplified cDNA. The ~1.8 kb-long amplification product obtained was cloned into pcDNA3.1 (Invitrogen) and pGH19 (kindly provided by Dr. Peter S. Aronson, Yale University) vectors such that the sense transcription of the cloned insert was under the control of T7 promoter. The identity of the cloned cDNA was confirmed by nucleotide sequencing.

2.2. Functional analysis of human SMCT2 in mammalian cells

This was done using the vaccinia virus expression system with human retinal pigment epithelial (HRPE) cells as described previously [13,15]. Uptake of L-[^{14}C]lactate, [^{14}C]nicotinate (both from American Radiolabeled Chemicals), and [^{14}C]pyruvate (Moravek Biochemicals) was measured in HRPE cells transfected with the cloned cDNA 15 h following transfection. The uptake medium contained 25 mM Hepes/Tris (pH 7.5), 140 mM NaCl, 5.4 mM KCl, 1.8 mM $CaCl_2$, 0.8 mM $MgSO_4$, and 5 mM glucose. When transport measurements were made in the absence of Na^+, NaCl in the uptake buffer was replaced with an equimolar concentration of *N*-methyl-D-glucamine (NMDG) chloride. Dose-response studies in which high concentrations of substrates as sodium salts were used, the concentration of NaCl in the uptake buffer was held constant at 100 mM and osmolarity maintained by the addition of appropriate concentrations of sodium gluconate. Endogenous uptake was measured in parallel using cells transfected with empty vector and subtracted from the corresponding uptake values measured in cells transfected with human SMCT2 cDNA to determine the cDNA-specific uptake. Uptake measurements were made in triplicate and experiments were repeated at least three times. Results are presented as means ± S.E.M. of these replicates. Statistical significance was analyzed by Student's t test.

2.3. Functional analysis of human SMCT2 in Xenopus laevis oocytes

Capped cRNA from human SMCT2 cDNA cloned in the pGH19 oocyte expression vector was synthesized using the mMESSAGE mMACHINE kit (Ambion). Mature oocytes from *X. laevis* were injected with 50 ng of cRNA and were used for uptake on the 5th day. Oocytes injected with water served as control. Uptake of radiolabeled substrates in control and SMCT2-expressing oocytes was determined as described previously [17]. Groups of 8–10 oocytes were incubated with 25 nM [^{14}C]nicotinate for 1 h at room temperature in NaCl-containing uptake buffer (100 mM NaCl, 2 mM KCl, 1 mM $MgCl_2$, 1 mM $CaCl_2$, 3 mM Hepes, 3 mM Mes, and 3 mM Tris, pH 7.5). At the end of 1 h, uptake was stopped by washing the oocytes 5 times with ice-cold uptake buffer. Subsequently, the oocytes were individually transferred to scintillation vials and lysed in 100 μl of 1% SDS/0.2 N NaOH and the radioactivity associated with each oocyte determined by liquid scintillation spectrometry. When the effect of the cation on the uptake was investigated, the NaCl in the uptake buffer was replaced with equimolar amounts of either KCl, LiCl, choline chloride or NMDG chloride. The Na^+-activation kinetics was analyzed by measuring human SMCT2-specific nicotinate uptake in the presence of increasing concentrations of Na^+. The data were analyzed by the Hill equation to determine the Hill coefficient (*h*; the number of Na^+ ions involved in the activation process). The kinetic parameters were determined using the computer software Sigma Plot, version 8.0 (Systat Software, Inc.) and the statistical significance of the data determined by Student's t test.

2.4. Generation of polyclonal antibody against SMCT2

A rabbit polyclonal anti-peptide antibody against mouse SMCT2 was raised by immunizing rabbits with the KLH-conjugated synthetic peptide GVQHDRETEQDYLD, which corresponds to amino acids 560–573 of mouse SMCT2. The antiserum obtained was affinity purified by passing through a NHS-activated HP column (Amersham Biosciences, Piscataway, NJ) in which the SMCT2-specific antigenic peptide used for immunization was coupled to NHS-activated sepharose. The specificity of the anti-SMCT2 antibody was confirmed by immunofluorescence in HRPE cells following heterologous expression of mouse and human

NIH-PA Author Manuscript

NIH-PA Author Manuscript

NIH-PA Author Manuscript

SMCT2 cDNAs by vaccinia virus-mediated expression. Cells transfected with pcDNA3.1 and mouse SMCT1 were used as the negative controls. Twelve hours after transfection, cells were fixed with 4% paraformaldehyde and incubated with the primary antibody at 1:2,000 dilution for 3 h at room temperature. Cells were subsequently washed with PBS and then incubated for 45 min at room temperature with Alexa Fluor 568-conjugated goat anti-rabbit secondary antibody. Cells were again washed, covered with Vectashield and coverslipped, and analyzed under a fluorescence microscope.

2.5. Immunolocalization of SMCT2 and SMCT1 in mouse kidney

Regional expression of SMCT2 and SMCT1 proteins in the mouse kidney was analyzed by immunofluorescence. The generation and specificity of rabbit polyclonal antibody against mouse SMCT1 has already been reported [18]. The fixation of mouse kidneys was performed as described by Bacic et al (19). Male C57BL6/J mice were anesthetized with ketamine and xylazine and subsequently fixed by vascular perfusion through the abdominal aorta. The fixative used for perfusion contained 3% paraformaldehyde, 0.5% picric acid, 0.01% glutardialdehyde in a 3:2 mixture of 0.1 M cacodylate buffer (pH 7.4, adjusted to 300 mosm with sucrose) and 4% hydroxyl ethyl starch (HES; Fresenius Kabi AG, Bad Homburg, Germany) in 0.9% NaCl. After 5 min, the fixative was washed out by perfusion with cacodylate/sucrose buffer for 5 min. Kidneys were removed and cut transversely into 2 mm slices which were subsequently mounted on thin cork plates. The slices were then frozen in liquid propane and stored at −80 °C until further use.

Consecutive slices of kidney tissue (5 μm) were obtained using a cryostat (CM1850, Leica, Wetzlar, Germany) and mounted on polylysine-coated microscope slides (O. Kindler, Freiburg, Germany). The cryosections were cut and dried at −20 °C for at least 12 h. When performing immunohistochemistry, the sections were rehydrated in phosphate-buffered saline (PBS) for 20 min before treating them for 3 min with 1% SDS in PBS. Following this antigen retrieval, the tissue was washed three times in PBS for 5 min each. For blocking nonspecific binding sites, the slides were incubated for 15 min with 1% bovine serum albumin (Sigma-Aldrich GmbH, Buchs, Switzerland) dissolved in PBS/0.02% sodium azide. The blocking solution was then carefully taken off and substituted by the primary antibodies which were diluted in PBS/0.02% sodium azide. Rabbit anti-SMCT2 and anti-SMCT1 antibodies were diluted 1:1000 and 1:4000, respectively. Goat anti-4F2hc (CD98) (Santa Cruz Biotechnologies, CA, USA) antibodies were applied at 1:400. Incubation time of the primary antibodies was 75 min, after which the slides were washed twice in hypertonic PBS and once in PBS for 5 min each. After washing, the secondary antibodies donkey anti-rabbit Alexa 594 (1:1000) and donkey anti-goat Alexa 488 (1:400) (Molecular Probes, OR, USA) were applied at room temperature and incubated for 1 h in the dark. Subsequent washing was performed as described before (19). After final washing, the sections were mounted with Vectashield mounting medium (Vector Laboratories, Burlingame, CA, USA) and subsequently stored in the dark at 4 °C. Microscopic images were taken using a Leica Confocal inverted microscope type XYZ (Leica, Wetzlar, Germany) and pictures were processed with Photoshop 7.0 software (Adobe, San Jose, CA).

3. Results

3.1. Structural features of the human SMCT2 cDNA and gene

The human SMCT2 cDNA, amplified by RT-PCR using human kidney mRNA, was 1,880 bp long and codes for a protein of 618 amino acids. During the preparation of this manuscript, two sequences for human SMCT2 with the accession numbers NM_001042366 and AY299482 have been annotated in the GenBank™ database. The nucleotide and the amino acid sequences of human SMCT2 that we cloned are identical to the sequences reported in the two submissions

NIH-PA Author Manuscript

NIH-PA Author Manuscript

NIH-PA Author Manuscript

to GenBank™. Comparison of the amino acid sequence between human SMCT2 and mouse SMCT2 (Fig. 1A) shows that the protein is highly conserved (85% identity and 92% similarity) between the two species. SMCT2 shares significant amino acid sequence homology with other members of the SLC5 gene family, especially SMCT1 (SLC5A8) (57% identity and 73% similarity) and NIS (SLC5A5) (48% identity and 66% similarity). A comparison of the nucleotide sequence of the genomic sequence entry NT_009237 in the GenBank™ database and the nucleotide sequence of the open reading frame of human SMCT2 cDNA indicated that the *SLC5A12* gene is ~50 kbp long and consists of 15 exons and 14 introns. The *SLC5A12* gene is mapped to chromosome 11p14.2 and the exon-intron organization of the gene is presented in Fig. 1B.

3.2. Functional features of human SMCT2 using a mammalian cell expression system

We expressed the cDNA in HRPE cells using the vaccinia virus expression technique and compared the uptake of lactate and pyruvate (Fig. 2A) and nicotinate (Fig. 2B) in cDNA-transfected cells with the uptake in cells transfected with the vector alone. The uptake of lactate, pyruvate and nicotinate was ~40% ($P < 0.05$), ~30% ($P < 0.05$), and ~200% ($p < 0.01$) higher, respectively, in cells expressing the cloned cDNA than in vector-transfected cells. Subsequent characterization of the cloned cDNA was done using radiolabeled nicotinate as the tracer. Uptake of nicotinate was measured in HRPE cells expressing human SMCT2 cDNA using uptake buffers in which NaCl was substituted with equimolar amounts of KCl or LiCl (Fig. 2C). Replacement of Na^+ in the uptake buffer with either K^+ or Li^+ almost completely abolished nicotinate uptake mediated by human SMCT2, indicating the obligatory nature of Na^+ as the coupling ion for human SMCT2.

Substrate affinities for human SMCT2 were determined by assessing the ability of unlabeled nicotinate, lactate and butyrate to inhibit the transport of [^{14}C]nicotinate in vector-transfected and human SMCT2 cDNA-transfected HRPE cells (Fig. 3A). In these experiments, the cDNA-specific uptake was calculated by subtracting the transport measured in vector-transfected cells and the IC_{50} values for nicotinate, lactate and butyrate were determined. The values were found to be in the following order: butyrate (2.6 ± 0.4 mM) > nicotinate (3.7 ± 0.6 mM) > lactate (16.9 ± 3.7 mM).

Previous studies from our laboratory have shown that non-steroidal anti-inflammatory drugs (NSAIDs) interact with human SMCT1 [20]. These studies have shown that NSAIDs are inhibitors, not transportable substrates, of human SMCT1. To investigate the interaction of NSAIDs with human SMCT2, we monitored the effects of some representative NSAIDs (200 μM) on human SMCT2-mediated [^{14}C]nicotinate transport. As seen in Fig. 3B, all NSAIDs tested inhibited human SMCT2-mediated nicotinate transport, suggesting that these drugs interacted with the transporter. The extent of inhibition, however, varied among the different drugs. Fenoprofen and ibuprofen showed similar extent of inhibition (54 ± 3 and 49 ± 4 %, respectively; $P < 0.01$). Inhibition by ketoprofen was the least (15 ± 3 %, $P < 0.05$).

3.3. Functional features of human SMCT2 using the X. laevis oocyte expression system

Since the human SMCT2-mediated transport activity following expression in HRPE cells was low, we explored the use of the *X. laevis* oocyte expression system. We first measured the uptake of [^{14}C]nicotinate in human SMCT2 cRNA-injected oocytes in the presence and absence of NaCl in the uptake buffer and compared it with the uptake measured in water-injected oocytes (Fig. 4A). Nicotinate uptake in human SMCT2 cRNA-injected oocytes was ~20 fold higher in cRNA-injected oocytes compared to water-injected oocytes. When NaCl in the buffer was substituted with chloride salt of K, Li, NMDG, or choline, nicotinate uptake decreased drastically and there was no significant difference in nicotinate uptake measured between cRNA-injected oocytes and water-injected oocytes. The uptake of [^{14}C]nicotinate was

NIH-PA Author Manuscript

NIH-PA Author Manuscript

NIH-PA Author Manuscript

completely inhibited by unlabeled nicotinate, lactate and butyrate (data not shown), suggesting that the uptake observed is specific and saturable and that human SMCT2 can interact with short-chain monocarboxylic acids. When the uptake of nicotinate was measured in the presence of the NSAIDs ibuprofen, fenoprofen and ketoprofen (200 μM), human SMCT2-mediated nicotinate uptake into cRNA-injected oocytes was significantly inhibited (Fig. 4B). The extent of inhibition was 76 ± 1% with ibuprofen, 67 ± 3% with fenoprofen and 45 ± 6% with ketoprofen (P <0.01 in all cases). The magnitude of inhibition obtained was relatively higher in the oocyte system, compared to the mammalian expression system (Fig. 3B). While the exact reason for the observed difference is difficult to predict, it is quite possible that the difference may be due to the differences in the various post-translational modifications the protein is subjected to in the two expression systems. The amino acid sequence of human SMCT2, in addition to putative N-linked glycosylation sites, also has several putative sites for phosphorylation and myristylation. Such post-translational modifications can affect the interaction of a transporter with its substrates/inhibitors. We next determined the Na^+-activation kinetics of human SMCT2-specific nicotinate uptake by measuring the uptake in the presence of increasing concentrations of Na^+ (0–100 mM). The concentration of Cl^- was kept constant at 100 mM. The relationship between uptake and Na^+ concentration was weakly sigmoidal (Fig. 4C). The value for the Hill coefficient (h) was slightly greater than 1 (1.4 ± 0.2) which was confirmed by the linear transformation of the data using the Hill plot (Fig. 4C, inset). However, electrophysiological studies with human SMCT2-expressing oocytes showed that the transport process was associated with barely detectable inward currents (< 5nA) in the presence of various substrates (data not shown).

3.4. Immunofluorescence localization of SMCT2 and SMCT1

To determine the regional and subcellular distribution of SMCT2 in kidney, we performed immunofluorescence analysis in mouse kidney sections. The anti-peptide antibody raised against the C-terminal portion of the transporter protein was affinity-purified and its specificity was confirmed using HRPE cells expressing the cloned transporters (data not shown). Positive immunofluorescence was obtained in cells expressing both human and mouse SMCT2, indicating that the antibody can interact with SMCT2 of both species. HRPE cells, which do not express SMCT2 endogenously, did not yield immunopositive signal when transfected with empty vector or human SMCT1 cDNA, confirming the specificity of the anti-SMCT2 antibody. To determine the exact localization of SMCT2 and SMCT1 in mouse kidney, double-labeling experiments were performed with antibodies against the 4F2hc (CD98) which is localized exclusively to the basolateral membrane of the early proximal tubule (21). Staining for SMCT2 and SMCT1 (red) was visible in the cortical region of the kidney consistent with their expression in the proximal tubule (Fig. 5). There were no immunopositive signals when the antibody was neutralized with the antigenic peptide before use (data not shown), attesting to the specificity of the antibody. The signals for SMCT2 or SMCT1 did not overlap with those of CD98, demonstrating that both transporters are localized to the brush border membrane (Fig 5A–D). Importantly, SMCT2 and SMCT1 showed a differential expression along the proximal tubule. SMCT2 was broadly expressed with the staining extending from the glomerulum, over the convoluted tubule (S1 and S2 segments) to the late proximal tubule (S3 segment). In contrast, SMCT1 staining was predominantly confined to tubular regions which had no CD98 signal, suggesting that SMCT1 expression is largely restricted to the late proximal tubule (straight proximal tubule, S3 segment). However, a faint signal for SMCT1 expression was visible in S2 segment of some nephrons.

4. Discussion

The studies presented here describe for the first time the functional features of human SMCT2. The cloned human SMCT2 functions as a Na^+-coupled transporter for lactate and other

NIH-PA Author Manuscript

NIH-PA Author Manuscript

NIH-PA Author Manuscript

monocarboxylates such as pyruvate, butyrate, and nicotinate. The substrate affinity of the transporter is much lower than that reported for human SMCT1 but similar to those described for the low-affinity Na^+-coupled lactate transport system in apical membrane vesicles from pars convoluta [6]. The immunolocalization of the transporter in mouse kidney agrees with the location of the low-affinity transport system. SMCT2 is expressed in the apical membrane of proximal convoluted tubule.

It is not clear at present whether the transport process mediated by human SMCT2 is electrogenic or not. The cooperativity of Na^+ activation of SMCT2 transport function is not robust as evident from the shallow nature of the sigmoidal relationship between Na^+ concentration and transport activity. Though a value of >1 for Hill coefficient suggests that the transport process may be electrogenic, substrate-induced inward currents under voltage-clamp conditions were barely detectable (< 5 nA) (data not shown). Mouse SMCT2 also induced only small inward currents (~10 nA) under similar conditions [15]. Recently, Plata et al [22] reported on the cloning and characterization of the zebrafish orthologs of SLC5A8 and SLC5A12. In their studies, they have conclusively demonstrated that SLC5A8 is an electrogenic transport system and SLC5A12 is an electroneutral transport system. Therefore, it is quite possible that mammalian SMCT2, similar to its ortholog in zebrafish, is an electroneutral transport system. The small magnitude of the currents observed with human SMCT2 and mouse SMCT2 suggests that these currents may not be directly coupled to solute transport.

The immunofluorescence studies with mouse kidney sections show that the low-affinity (SMCT2) and high-affinity (SMCT1) lactate transporters are present in the apical membrane. The expression of SMCT2 is evident all through the entire length of the proximal tubule (S1/S2/S3 segments) whereas the expression of SMCT1 is mostly restricted to the straight portions of the proximal tubule (S3 segment). Though the anti-SMCT2 antibody was able to interact with human SMCT2 in transfected cells, our attempts to use the antibody to localize SMCT2 in human kidney sections resulted in high nonspecific staining. We believe that the distribution for SMCT2 and SMCT1 in human kidney would be similar to that in mouse kidney; however, interspecies differences have been observed with respect to the localization and expression of transporters, e.g., organic cation transporters [23]. The differential distributions of high-affinity and low-affinity lactate transporters in various segments of the proximal tubule is similar to what has been reported for the high-affinity and low-affinity Na^+-dependent transporters for glucose [24] and H^+-dependent transporters for peptides [25]. This expression pattern of SMCT2 and SMCT1 in the proximal tubule has physiologic significance in terms of lactate reabsorption in the kidney. The concentration of lactate is quite high, equal to the concentration found in plasma, in the lumen of the early parts of the proximal convoluted tubule. SMCT2 is expressed in this region. This transporter, being a low-affinity type, would be able to mediate the reabsorption of lactate very effectively under these conditions. As lactate reabsorption progresses via SMCT2, the luminal concentration of lactate would fall along the proximal tubule. SMCT1 is expressed in the straight portions of the proximal tubule. This transporter, being a high-affinity type, would be able to carry out the reabsorption process effectively under these conditions. Thus, the two transporters could work in tandem in the proximal tubule, contributing to the efficient reabsorption of lactate.

We believe that SMCT1 and SMCT2 are the only transporters that are responsible for the transfer of lactate from the tubular lumen into the cells across the apical membrane in the proximal tubule. Recently, we reported that the expression of both these transporters is almost completely abolished in a mouse model in which the gene coding for the transcription factor c/ebpδ had been disrupted [16]. In this mouse model, the urinary excretion of lactate is markedly increased, with consequent decrease in plasma levels of lactate compared to wild type mice. The plasma levels of lactate in c/ebpδ null mice are only about 5% of control values.

NIH-PA Author Manuscript

NIH-PA Author Manuscript

NIH-PA Author Manuscript

These findings with c/ebp∂ null mice provide convincing in vivo evidence for the obligatory role of SMCT1 and SMCT2 in lactate reabsorption in the kidney.

References

1. Hohmann B, Frohnert PP, Kinne R, Baumann K. Proximal tubular lactate transport in rat kidney: a micropuncture study. Kidney Int 1974;5:261–270. [PubMed: 4853933]
2. McKelvie RS, Lindinger MI, Heigenhauser GJ, Sutton JR, Jones NL. Renal responses to exercise-induced lactic acidosis. Am J Physiol 1989;257:R102–108. [PubMed: 2750954]
3. Poole RC, Halestrap AP. Transport of lactate and other monocarboxylates across mammalian plasma membranes. Am J Physiol 1993;264:C761–782. [PubMed: 8476015]
4. Barac-Nieto M, Murer H, Kinne R. Lactate-sodium cotransport in rat renal brush border membranes. Am J Physiol 1980;239:F496–506. [PubMed: 6159793]
5. Wright EM. Transport of carboxylic acids by renal membrane vesicles. Annu Rev Physiol 1985;47:127–141. [PubMed: 3888071]
6. Jorgensen KE, Sheikh MI. Renal transport of monocarboxylic acids. Heterogeneity of lactate-transport systems along the proximal tubule. Biochem J 1984;223:803–807. [PubMed: 6508742]
7. Jorgensen KE, Sheikh MI. Mechanisms of uptake of ketone bodies by luminal-membrane vesicles. Biochim Biophys Acta 1985;814:23–34. [PubMed: 3978098]
8. Jorgensen KE, Sheikh MI. Characteristics of uptake of short chain fatty acids by luminal membrane vesicles from rabbit kidney. Biochim Biophys Acta 1986;860:632–640. [PubMed: 3741867]
9. Jorgensen KE, Sheikh MI. Transport of pyruvate by luminal membrane vesicles from pars convoluta and pars recta of rabbit proximal tubule. Biochim Biophys Acta 1988;938:345–352. [PubMed: 3349069]
10. Miyauchi S, Gopal E, Fei YJ, Ganapathy V. Functional identification of SLC5A8, a tumor suppressor down-regulated in colon cancer, as a Na^+-coupled transporter for short-chain fatty acids. J Biol Chem 2004;279:13293–13296. [PubMed: 14966140]
11. Gopal E, Fei YJ, Sugawara M, Miyauchi S, Zhuang L, Martin P, Smith SB, Prasad PD, Ganapathy V. Expression of slc5a8 in kidney and its role in Na^+-coupled transport of lactate. J Biol Chem 2004;279:44522–44532. [PubMed: 15322102]
12. Coady MJ, Chang MH, Charron FM, Plata C, Wallendorff B, Sah JF, Markowitz SD, Romero MF, Lapointe JY. The human tumour suppressor gene SLC5A8 expresses a Na^+-monocarboxylate cotransporter. J Physiol 2004;557:719–731. [PubMed: 15090606]
13. Gopal E, Fei YJ, Miyauchi S, Zhuang L, Prasad PD, Ganapathy V. Sodium-coupled and electrogenic transport of B-complex vitamin nicotinic acid by slc5a8, a member of the Na^+/glucose co-transporter gene family. Biochem J 2005;388:309–316. [PubMed: 15651982]
14. Ganapathy V, Gopal E, Miyauchi S, Prasad PD. Biological functions of SLC5A8, a candidate tumour suppressor. Biochem Soc Trans 2005;33:237–240. [PubMed: 15667316]
15. Srinivas SR, Gopal E, Zhuang L, Itagaki S, Martin PM, Fei YJ, Ganapathy V, Prasad PD. Cloning and functional identification of slc5a12 as a sodium-coupled low-affinity transporter for monocarboxylates (SMCT2). Biochem J 2005;392:655–664. [PubMed: 16104846]
16. Thangaraju M, Ananth S, Martin PM, Roon P, Smith SB, Sterneck E, Prasad PD, Ganapathy V. c/ebp∂ null mouse as a model for the double-knockout of slc5a8 and slc5a12 in kidney. J Biol Chem 2006;281:26769–26773. [PubMed: 16873376]
17. Miyauchi S, Srinivas SR, Fei YJ, Gopal E, Umapathy NS, Wang H, Conway SJ, Ganapathy V, Prasad PD. Functional characteristics of NaS2, a placenta-specific Na^+-coupled transporter for sulfate and oxyanions of the micronutrients selenium and chromium. Placenta 2006;27:550–559. [PubMed: 16129486]
18. Martin PM, Gopal E, Ananth S, Zhuang L, Itagaki S, Prasad BM, Smith SB, Prasad PD, Ganapathy V. Identity of SMCT1 (SLC5A8) as a neuron-specific Na^+-coupled transporter for active uptake of L-lactate and ketone bodies in the brain. J Neurochem 2006;98:279–288. [PubMed: 16805814]
19. Bacic D, Lehir M, Biber J, Kaissling B, Murer H, Wagner CA. The renal Na^+/phosphate cotransporter NaPi-IIa is internalized via the receptor-mediated endocytic route in response to parathyroid hormone. Kidney Int 2006;69:495–503. [PubMed: 16514432]

NIH-PA Author Manuscript

NIH-PA Author Manuscript

NIH-PA Author Manuscript

20. Itagaki S, Gopal E, Zhuang L, Fei YJ, Miyauchi S, Prasad PD, Ganapathy V. Interaction of ibuprofen and other structurally related NSAIDs with the sodium-coupled monocarboxylate transporter SMCT1 (SLC5A8). Pharm Res 2006;23:1209–1216. [PubMed: 16729224]

21. Rossier G, Meier C, Bauch C, Summa V, Sordat B, Verrey F, Kuhn LC. LAT2, a new basolateral 4F2hc/CD98-associated amino acid transporter of kidney and intestine. J Biol Chem 1999;274:34948–34954. [PubMed: 10574970]

22. Plata C, Sussman CR, Sindic A, Liang JO, Mount DB, Josephs ZM, Chang MH, Romero MF. Zebrafish Slc5a12 encodes an electroneutral sodium monocarboxylate transporter (SMCTn): A comparison to the electrogenic SMCT (SMCTe/Slc5a8). J Biol Chem 2007;282:11996–12009. [PubMed: 17255103]

23. Motohashi H, Sakurai Y, Saito H, Masuda S, Urakami Y, Goto M, Fukatsu A, Ogawa O, Inui K. Gene expression levels and immunolocalization of organic ion transporters in the human kidney. J Am Soc Nephrol 2002;13:866–874. [PubMed: 11912245]

24. Wright EM. Renal Na^+-glucose cotransporters. Am J Physiol Renal Physiol 2001;280:F10–18. [PubMed: 11133510]

25. Shen H, Smith DE, Yang T, Huang YG, Schnermann JB, Brosius FC. 3rd, Localization of PEPT1 and PEPT2 proton-coupled oligopeptide transporter mRNA and protein in rat kidney. Am J Physiol 1999;276:F658–665. [PubMed: 10330047]

NIH-PA Author Manuscript

NIH-PA Author Manuscript

NIH-PA Author Manuscript

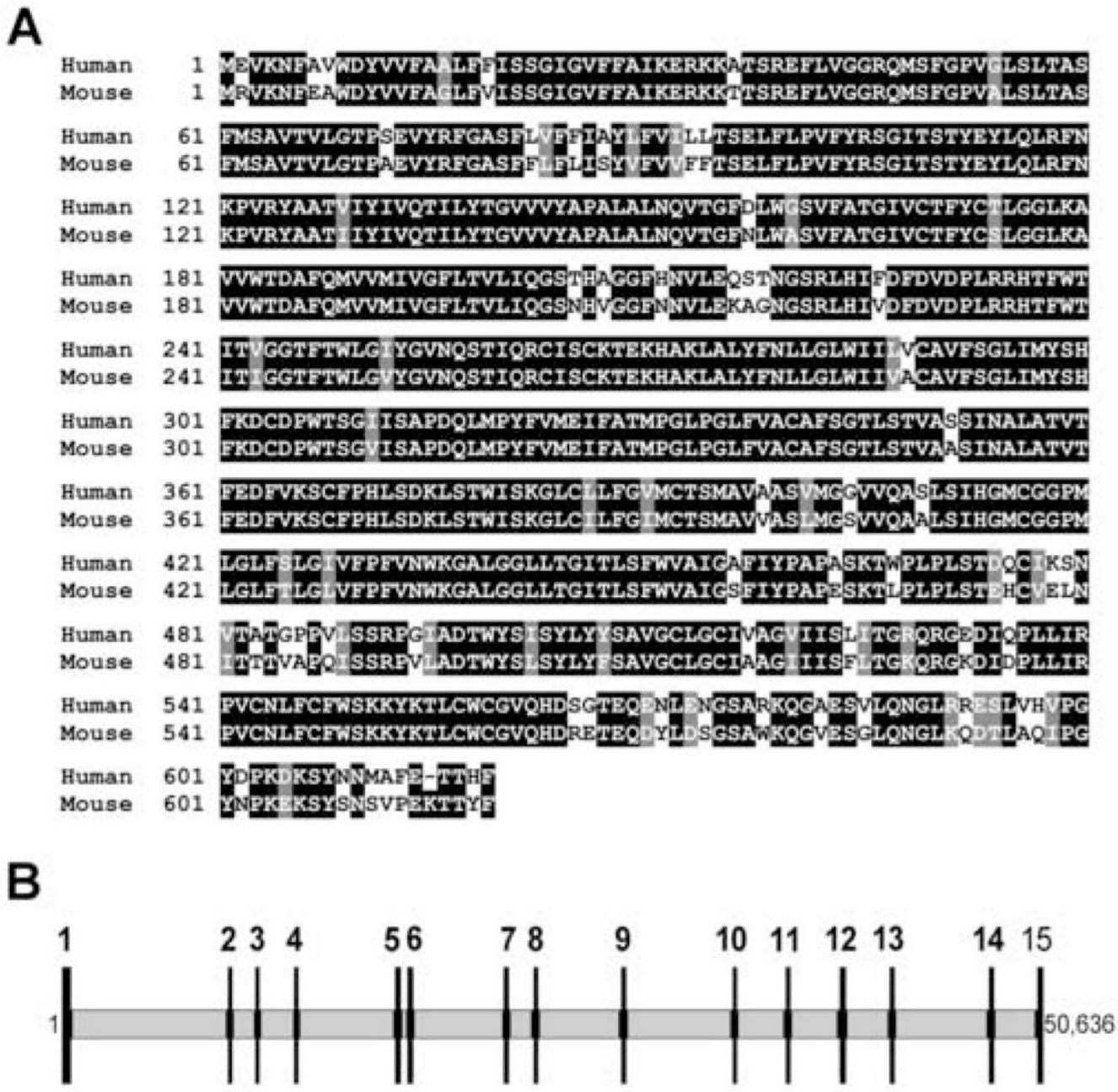

Fig. 1.

Fig. 1A. Comparison of the amino acid sequences of human SLC5A12 with that of mouse slc5a12. Identical amino acids are shaded dark and conservative substitutions are shaded light. Fig. 1B. Exon-intron organization of human *SLC5A12* gene. Black boxes numbered 1–15 represent the exons and the shaded regions represent the introns.

NIH-PA Author Manuscript

NIH-PA Author Manuscript

NIH-PA Author Manuscript

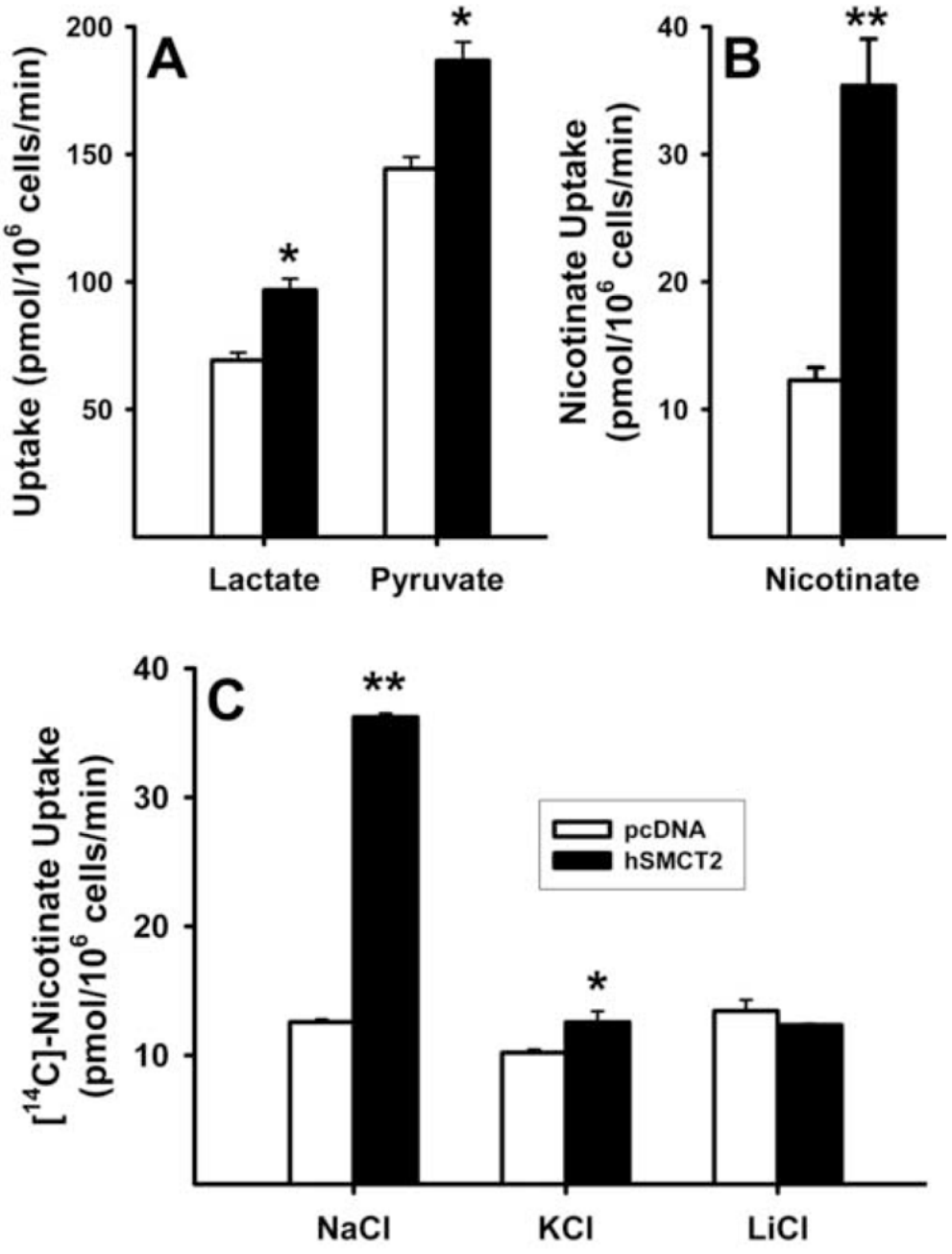

Fig. 2.

Functional expression of human SMCT2 (SLC5A12) in HRPE cells. HRPE cells were transfected with either pcDNA3.1 vector alone (open bars) or human SMCT2 cDNA (closed bars). (**A, B**) Uptake of [^{14}C]lactate (500 μM), [^{14}C]pyruvate (500 μM), and [^{14}C]nicotinate (30 μM) was measured in the presence of Na^+. (**C**) Uptake of [^{14}C]nicotinate was measured either in control buffer (25 mM Hepes/Tris, pH 7.5, 5.4 mM KCl, 1.8 mM $CaCl_2$, 0.8 mM $MgSO_4$, 5 mM glucose, and 140 mM NaCl) or in buffer in which NaCl was replaced with 140 mM of KCl or LiCl. Where indicated, uptake measured in cDNA-transfected cells was significantly different from the corresponding uptake measured in vector-transfected cells (*$P < 0.05$; **$P < 0.01$).

NIH-PA Author Manuscript
NIH-PA Author Manuscript
NIH-PA Author Manuscript

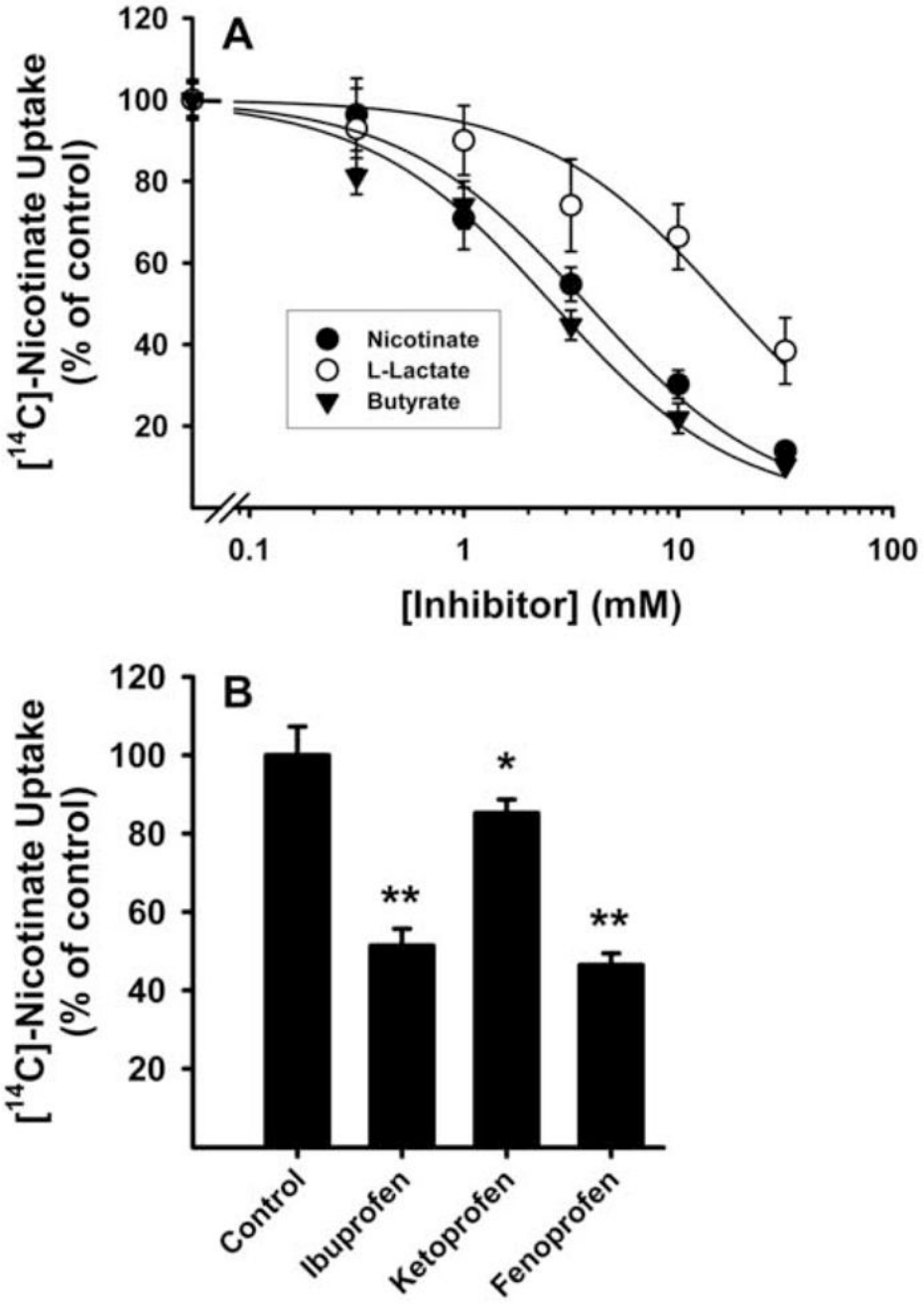

Fig. 3.

Dose-response relationship for the inhibition of human SMCT2-mediated [^{14}C]nicotinate uptake by unlabeled nicotinate, lactate, and butyrate (A) and inhibition of human SMCT2-mediated nicotinate uptake by NSAIDs (B). Human SMCT2 cDNA was expressed in HRPE cells. Cells transfected with pcDNA3.1 vector served to determine endogenous transport. Uptake of [^{14}C]nicotinate (30 μM) was measured in Na^+-containing buffer either in the presence of increasing concentrations of unlabelled nicotinate, L-lactate, or butyrate (A) or various NSAIDs (200 μM) (B). Uptake measured in cells transfected with vector alone was subtracted from corresponding uptake measured in cells transfected with cDNA to calculate cDNA-specific uptake. Results are expressed as percentage of control uptake (100 %)

NIH-PA Author Manuscript

NIH-PA Author Manuscript

NIH-PA Author Manuscript

measured in the absence of inhibitors. The degree of statistical significance for nicotinate uptake measured in the presence of NSAIDs compared to nicotinate uptake measured in the absence of various NSAIDs in hSMCT2 cDNA-transfected cells is indicated by $*P < 0.05$ and $** P < 0.01$.

NIH-PA Author Manuscript
NIH-PA Author Manuscript
NIH-PA Author Manuscript

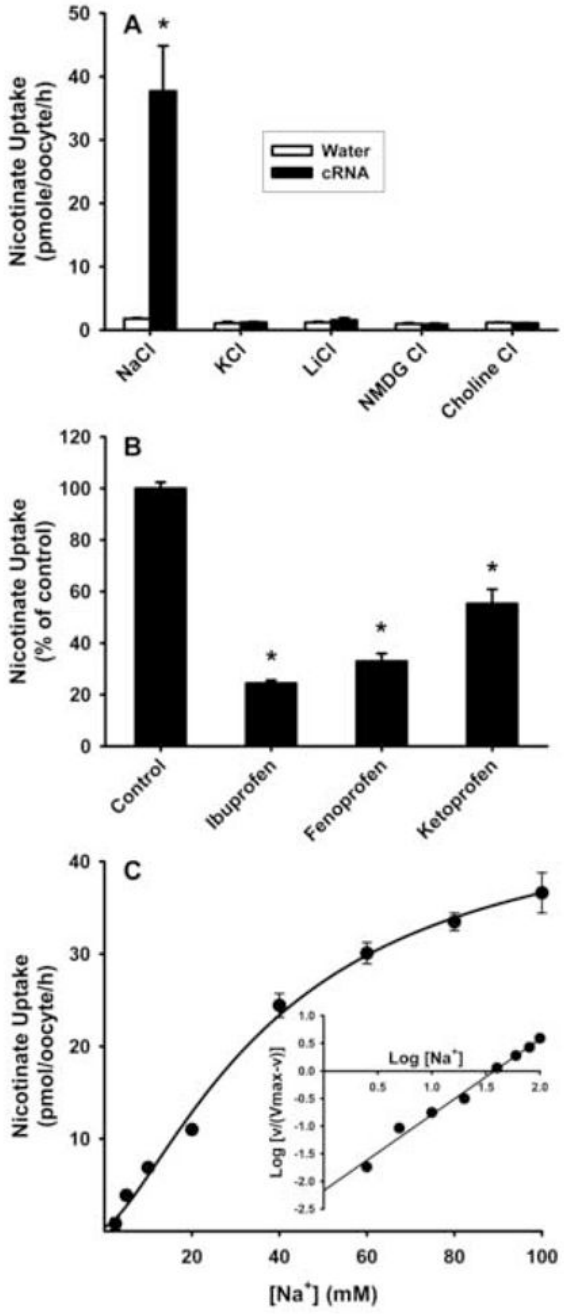

Fig. 4.

Characterization of human SMCT2-mediated transport process in *Xenopus* oocytes. Oocytes were injected with either human SMCT2 cRNA or water and used for the measurements of [^{14}C]nicotinate (25 μM) uptake on the 5th day. Uptake measured under identical conditions in water-injected oocytes was subtracted from uptake in cRNA-injected oocytes to calculate human SMCT2-specific uptake. (A) Cation specificity of human SMCT2-mediated transport. Uptake was measured in control buffer (100 mM NaCl, 2 mM KCl, 1 mM $CaCl_2$, 1 mM $MgCl_2$, 3 mM Hepes, 3 mM Mes, and 3 mM Tris, pH 7.5) or in buffer in which NaCl was replaced with 100 mM of KCl, LiCl, choline chloride or NMDG chloride. The degree of statistical significance for uptake measured in cRNA-injected oocytes compared to hSMCT2

NIH-PA Author Manuscript

NIH-PA Author Manuscript

NIH-PA Author Manuscript

water-injected oocytes is indicated by * P <0.01. (B) Influence of NSAIDs on human SMCT2-mediated nicotinate uptake. Uptake of [^{14}C]nicotinate was measured in the absence (control) or presence of 200 μM of various NSAIDs. Uptake measurements were made in a medium containing 100 mM Na^+. The degree of statistical significance for nicotinate uptake measured in the presence of NSAIDs compared to nicotinate uptake measured in the absence of various NSAIDs in hSMCT2 cRNA-injected oocytes is indicated by *P < 0.01. (C) Na^+-activation kinetics for human SMCT2-mediated nicotinate uptake. Uptake of nicotinate was measured in the presence of increasing concentrations of Na^+ (0–100 mM). Concentration of Cl^- was kept constant at 100 mM. Na^+-dependent uptake was calculated by subtracting the uptake measured in the absence of Na^+ from the uptake measured in the presence of Na^+. Data for the Na^+-dependent uptake were used in the analysis. *Inset*, Hill plot of the same data.

NIH-PA Author Manuscript
NIH-PA Author Manuscript
NIH-PA Author Manuscript

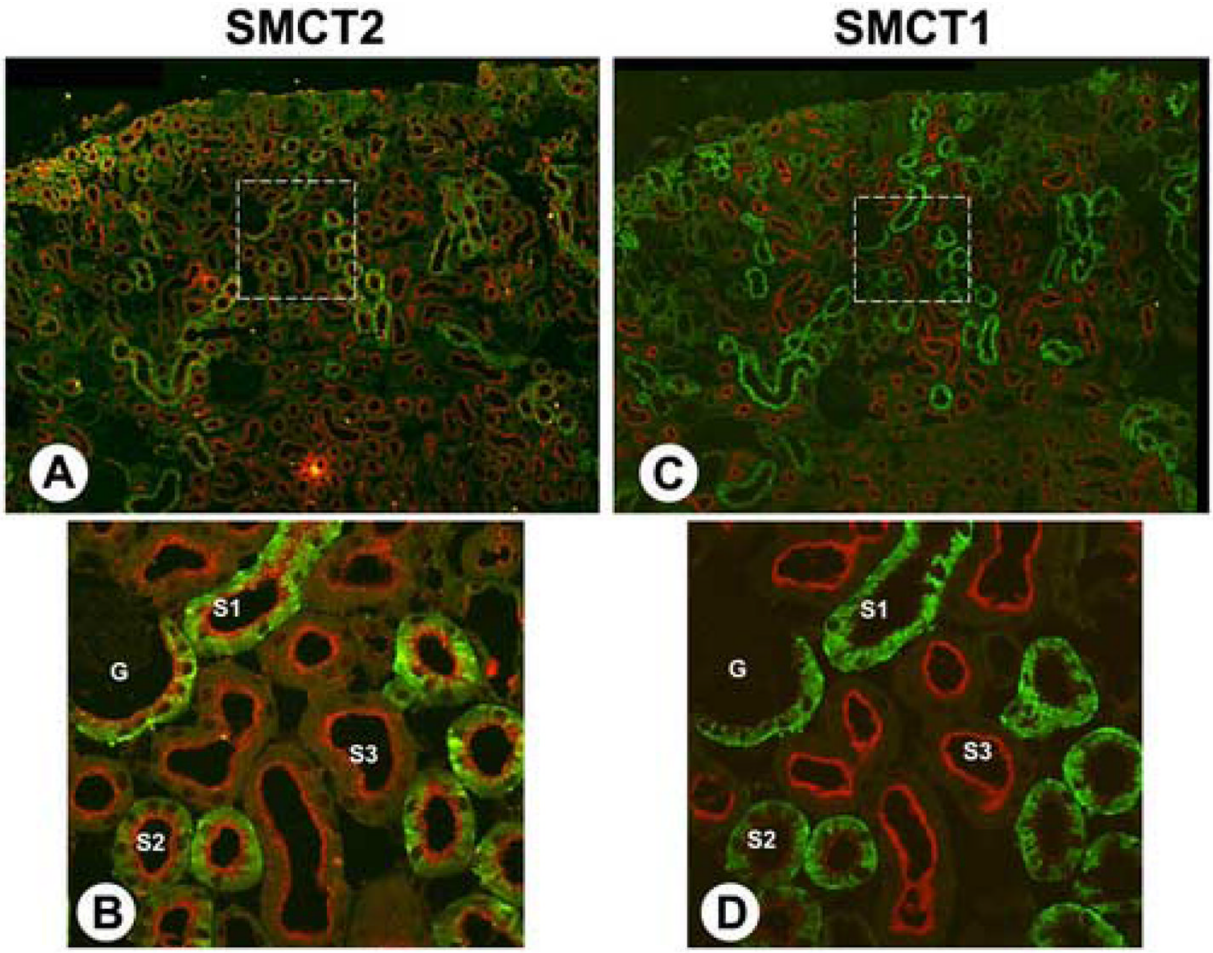

Fig. 5.

Immunolocalization of SMCT2 and SMCT1 in mouse kidney. Consecutive cryosections of mouse kidney were stained with rabbit polyclonal antibodies specific for SMCT2 or SMCT1 (red) together with an anti-4F2hc (CD98) antibody (green). Panels A and C: Cortical sections (original magnification 200 x), demonstrating strong staining for SMCT2 and SMCT1 in different segments of the proximal tubule. Panels B and D: high magnification confocal laser microscope images (original magnification 630 x), showing localization of SMCT2 and SMCT1 in the brush border membrane of the proximal tubule. (B) SMCT2 staining was observed along the entire proximal tubule localizing not only to the CD98-positive segments (S1 and S2) but also to the CD98-negative segments (S3). (D) SMCT1 staining was absent from proximal tubular segments positive for CD98 (S1) but was present in CD98-negative segments (S3). A faint signal was visible in some S2 segments. G, glomerulum; S1 and S2, early and late convoluted proximal tubule, respectively; S3, straight part of the proximal tubule.